

## THE EFFECT OF PERMAFROST ON THE IP RESPONSE OF LEAD ZINC ORES<sup>1</sup>

ANTHONY KAY<sup>2</sup> AND K. DUCKWORTH<sup>3</sup>

### ABSTRACT

A major concern when performing an Induced Polarization (IP) survey in arctic and subarctic regions is the effect of permafrost on the electrical properties of mineralized rocks. The present study compares the IP response on a suite of rock samples measured at two temperatures,  $25 \pm 1^\circ\text{C}$  and  $-14 \pm 1^\circ\text{C}$ .

Complex resistivity measurements were obtained from four sulphide ore samples which were selected from three different deposits: the Hawk Creek orebody, British Columbia, the Pine Point deposit, Northwest Territories, and the Arvik deposit on Little Cornwallis Island, N.W.T.

The results obtained from measurements on mineralized rock specimens indicated that the effect of low temperature was to increase the chargeability and time constant parameters of the IP response. Changes in the porosity and tortuosity of the rock specimens at a temperature below  $0^\circ\text{C}$  appear to be responsible for the observed changes in the IP response.

### INTRODUCTION

The electrical characteristics of metallic mineral deposits have been studied by a number of authors, among them being Pelton *et al.* (1978), Klein and Hallof (1982), Van Voorhis *et al.* (1973) and Zonge *et al.* (1972).

The study we report here provides an extension of these earlier studies, with particular emphasis on the change in electrical character of metallic mineral specimens as their temperature is lowered to simulate permafrost conditions.

The Cole-Cole equivalent circuit concept described by Pelton *et al.* (*ibid.*) was used throughout this study as the means of characterizing the electrical properties of minerals. The basis for this concept is that the frequency dependence of the electrical properties of a rock can be simulated exactly by a simple equivalent circuit of the type shown in Figure 1. The dispersive characteristics of such a circuit, and therefore of a rock specimen or of a body of rock *in situ*, or even of a single

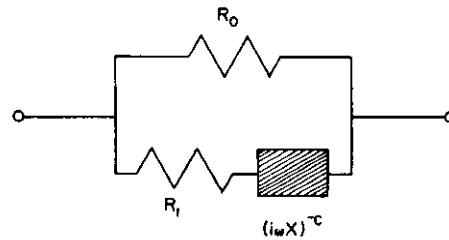


Fig. 1. Equivalent circuit for a mineralized rock.

mineral interface that the circuit simulates, can be specified by four parameters: the DC resistance  $R_0$ , the chargeability  $m$ , the time constant  $\tau$  and the frequency dependence  $c$ . When employed in the following expression, these four parameters provide a complete description of the impedance or transfer function  $Z(\omega)$  of the equivalent circuit and the rock being tested.

$$(1) \quad Z(\omega) = R_0 \left[ 1 - m \left\{ 1 - \frac{1}{1 + (i\omega\tau)^c} \right\} \right]$$

These four parameters can be described in terms of the features of the equivalent circuit of Figure 1 as follows:

- $R_0$  is the resistance of the circuit at zero frequency.
- $m$  is the resistance difference between zero and infinite frequency, normalized with respect to the zero frequency resistance, *i.e.*  
 $m = R_0 / (R_1 + R_0)$
- $\tau$  is the decay time constant of the circuit in response to a current step function  
 $(\tau = X(R_0/m)^{1/c} = X(R_1 + R_0)^{1/c}$   
 where  $X$  is a constant.)
- $c$  is the frequency dependence, which has no physical significance in the equivalent circuit but which is dependent on the texture of the rock being studied.
- $\omega$  is angular frequency (*i.e.*  $\omega = 2\pi f$ )

<sup>1</sup>Paper presented at the C.S.E.G. National Convention, Calgary, April 1982

<sup>2</sup>Hardy Associates (1978) Ltd., Calgary, Alberta

<sup>3</sup>Dept. of Geology/Geophysics, The University of Calgary, Calgary, Alberta

The authors gratefully acknowledge the assistance and cooperation of the following individuals and organizations: W.J. Scott of Hardy Associates (1978) Ltd., L.S. Collett of the Geological Survey of Canada, Cominco Ltd., and the Department of Indian and Northern Affairs.

This study was supported by grants from the Natural Science Engineering Research Council, and with equipment loaned from the Geological Survey of Canada.

In presenting the impedance versus frequency spectrum (*i.e.* the transfer function) of a rock or its equivalent circuit, expression (1) must be re-expressed in terms of its amplitude and phase, which may be shown to be given by (Kay, 1981):

(2)

$$|z| = R_0 \left[ \left\{ 1 - m \left( 1 + \frac{1 + (w\tau)^c \cos(\pi c/2)}{1 + 2(w\tau)^c \cos(\pi c/2) + (w\tau)^{2c}} \right) \right\}^2 + \left\{ m \left( \frac{(w\tau)^c \sin(\pi c/2)}{1 + 2(w\tau)^c \cos(\pi c/2) + (w\tau)^{2c}} \right) \right\}^2 \right]^{1/2}$$

(3)

$$\Phi = \text{Arctan} \left[ \frac{(1-m) \{ 1 + 2(w\tau)^c \cos(\pi c/2) + (w\tau)^{2c} \} + m \{ 1 + (w\tau)^c \cos(\pi c/2) \}}{m(w\tau)^c \sin(\pi c/2)} \right]$$

When plotted against frequency, with arbitrarily nominated values for the four parameters, expressions (2) and (3) generate an impedance spectrum of the form shown in Figure 2. This shows the general character of all such plots, in that the amplitude declines toward higher frequencies and the phase peaks at some frequency which is called the characteristic or critical frequency of the circuit or rock. It should be noted that all phase values are negative but are plotted to display the minimum as a peak.

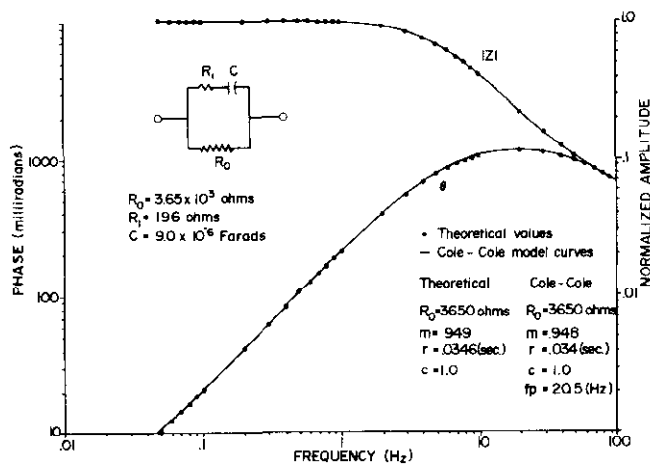


Fig. 2. Equivalent circuit and frequency response with Cole-Cole model.

#### METHOD OF STUDY

Specimens were collected from three lead-zinc ore occurrences of the Mississippi Valley type, in which galena sphalerite and marcasite are the predominant minerals. The first site was located in Little Cornwallis Island in the Arctic, the second was at Pine Point in the Northwest Territories and the third at Hawk Creek in Kootenay National Park on the Alberta - British Columbia border. These sites were chosen for their similarity in mineralization, with a view to following the laboratory study of specimens with an *in situ* study of the ore.

It was hoped that the character of the three sets of samples would prove electrically uniform, so that any differences between *in situ* results from the temperate and permafrost sites could be attributed to the effect of permafrost. This uniformity was not observed, so *in situ* tests seeking this effect would probably not be conclusive.

The equipment used in the laboratory study of these specimens is illustrated in block-diagram form in Figure 3. The Hunttec Mk4 IP field recording and processing receiver was used in the hope that procedures and data-processing software developed in these studies could also be used in the proposed *in situ* tests.

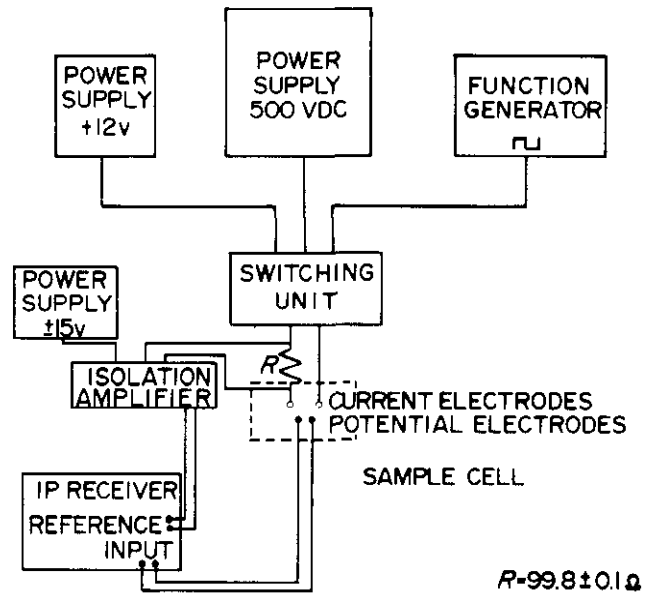


Fig. 3. Schematic diagram of the laboratory apparatus.

The current switching unit was specially developed for the project, in order to provide the frequency precision demanded by the Hunttec Mk4. Timing control was provided by means of a Hewlett Packard 3324A signal generator while reference signals were supplied to the receiver by way of an Intronic IA286 isolation amplifier.

The procedure for obtaining the impedance spectrum of a rock specimen involved the digital recording of the voltage signals developed across the specimen in response to a square-wave current input over a frequency range from 0.0156 Hz to 16 Hz. This record was then Fourier transformed to be presented in the form shown in Figure 2. Although the transformation could be achieved by software built into the Mk4 receiver, alternative processing was developed which involved transferring the digital record from the Hunttec Mk4 to a Honeywell Multics computer by means of a cassette tape. This alternative processing was designed to allow full use of the recording capability of the Hunttec Mk4, which permits both the current-input and the voltage-input waveforms from a sample (or from a field record) to be recorded. These two waveforms can then be deconvolved to obtain the transfer function of the rock (*i.e.* the type

of function shown by Fig. 2). The software provided in the Mk4 assumes the current waveform to be a perfect square wave, which may not be the case under field operating conditions, so that the internal software may give erroneous results in such circumstances. In the laboratory we were able to ensure that the current waveform was accurately square, so the internal processing of the Mk4 was used there.

After a spectrum had been produced by this process, the four Cole-Cole parameters for that spectrum were obtained by fitting the observed data points with curves generated by an algorithm based on expressions (2) and (3). The process of fitting required iterative modification of the four parameters until a fit was achieved. The iteration process was under the control of the operator rather than automatic.

The type of test cell into which each rock specimen was mounted for these studies is shown in Figure 4. It consisted of a rectangular plexiglass tank (dimensions 20 cm × 10 cm × 8 cm) with graphite plates at each end of the tank acting as current electrodes. The rock specimens were cut into rectangular slab form, so that they were a close fit in the tank when mounted as shown. A watertight seal between the specimen and the tank walls was achieved by a layer of silicon grease; this prevented current flow around the edges of the specimen. Potential measurements were made by means of a pair of Luggin capillary-type electrodes, the tips of which could be placed anywhere in the plexiglass tank. Normally the electrode tips were placed close to the faces of the rock specimen. Polarization effects due to the graphite electrodes could be observed if the potential electrodes were placed close to them (*i.e.* within 1 cm), but in normal conditions each potential electrode was located more than 5 cm from either of the current electrodes.

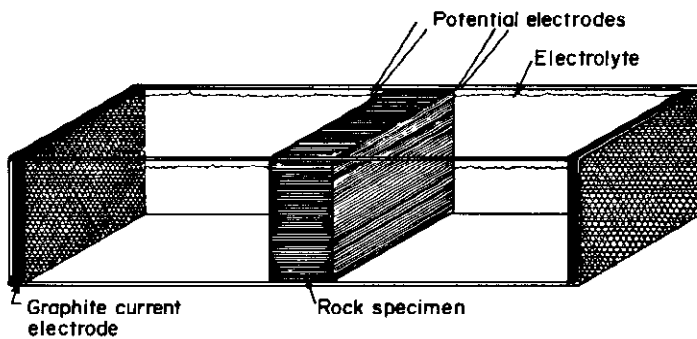


Fig. 4. Test cell.

Two electrolytes were used to saturate the rock specimens: untreated tapwater and a 0.1 N solution of NaCl. It was decided that no benefit was likely to be derived from the use of distilled water in place of tap water, because the aim was simply to increase the salinity of the pore fluid. The presence of original fluids rendered any attempt to achieve an accurately measurable change of salinity impossible.

Each specimen was tested first while saturated with tap water; then, after oven drying. It was resaturated with the salt solution. Repeated saturation with distilled water might have removed original fluids and their dissolved salts, but could also have altered the rock.

Tests were conducted at two stable temperatures, 25°C and -14°C, with no attempt made to take measurements while the temperature of the test cell was being lowered. The low-temperature tests were conducted with the whole test cell placed inside a domestic freezer.

An inevitable problem in the low-temperature measurements was that the test-cell fluid outside the specimen had to remain unfrozen, yet had also to have the composition of the pore fluids of the specimen. Our only remedy was to cool the specimen and tank to -14°C without the main body of electrolyte, and to add the electrolyte immediately before the experiment. This procedure led to some difficulties in maintaining the saturation of the rock specimens, and with the warming of the specimen by the introduced electrolyte. It was expected that this warming would affect the  $R_0$  parameter and thus also the amplitude of the impedance spectrum. The absence of  $R_0$  from expression (3) for phase suggested that slight warming of the faces of the sample would not have a strong influence on the phase spectrum, and this proved to be the case.

The electrolyte was at room temperature when introduced into the tank. This was necessary because, if the electrolyte had been added at just above its freezing point, the whole tank would have become frozen before the experiment on any one specimen could have been completed. Each set of measurements on one rock sample took between 15 and 20 minutes.

#### TESTS OF EQUIPMENT AND PROCEDURES

A variety of tests were employed to ensure that the measurement system performed as expected.

The results of a test in which a purely resistive load replaced the sample cell are shown on curve A of Figure 5. The error bars denote plus and minus one standard deviation from the mean of as many as ten readings taken at each of the eleven fundamental frequencies that can be treated by the Hunttec Mk4 receiver. Only the phase results are shown, because the amplitude values were constant for all frequencies to within  $\pm 1\%$ . Amplitude and phase values for the higher-order harmonics of these fundamental frequencies can be provided by the Hunttec Mk4, but were not used because they proved significantly less accurate than the results measured at the available fundamental frequencies. In no case did the measured mean phase deviate by more than 3 milliradians from the expected value of zero milliradians for this purely resistive case. This systematic error was treated as being negligible in the measurements on the mineralized rocks.

The results for a test in which the specimen cell was loaded only with electrolyte are shown in curve B of

Figure 5. This test might have been expected to duplicate the behaviour of the purely resistive load, but a consistent systematic difference from that behaviour is clear in curves A and B. This deviation was probably due to polarization of the current-supply electrodes in the test cell but, even so, the effect was small enough to be insignificant to the measurements made on the mineralized specimens.

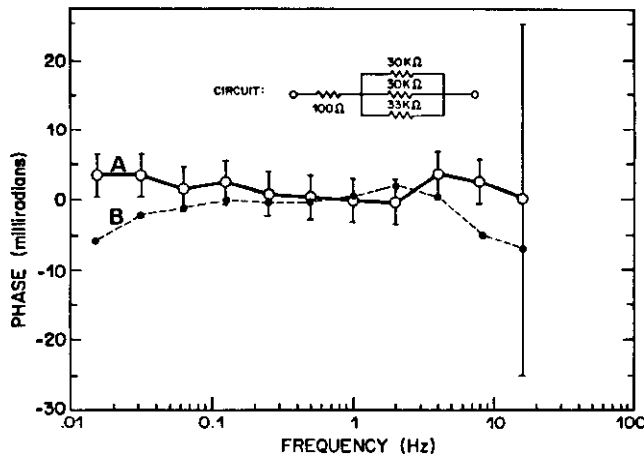


Fig. 5. Phase response of the resistor network (curve A) and of the sample cell containing only electrolyte (curve B).

In order to test the ability of the system to handle a specimen that was significantly polarizable, it was applied to measurements of the behaviour of a simple R-C circuit. The results of this test are shown in Figure 6, along with the theoretical phase curve for that R-C circuit. The agreement between the observed fundamental frequency data points and the theoretical phase curve appears to lie within the error limits for all frequencies shown in Figure 5. However, the data values obtain from the 3rd and higher harmonics of each of the fundamental frequencies (shown as uncircled points in Figure 6) showed systematic deviations from the theoretical curve. These deviations are exaggerated by the logarithmic scale at low frequencies in Figure 6. As mentioned earlier, these harmonic values were not used in assembling spectra from rock samples.

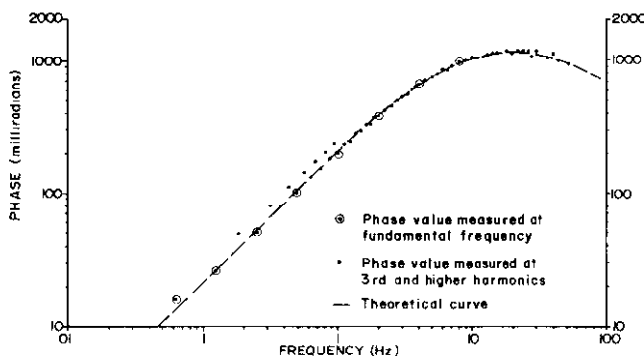


Fig. 6. Phase response of the RC network measured with the Mark IV receiver.

A test of the Cole-Cole curve matching program, when applied to the data measured from the R-C circuit shown in Figure 6, showed that the Cole-Cole parameters derived by matching differed from the theoretical values by no more than 2% in the worst case.

A test of linearity was performed by measuring the impedance spectrum for a synthetic rock specimen over a range of current densities. It was found that linearity held for current densities up to  $1.8 \times 10^{-2}$  A/m<sup>2</sup>, so all measurements on the rock specimens were conducted with current densities well below this value.

## RESULTS

The results presented here are for a selection of four specimens characterized as follows:

PPM: Calcite Marcasite. Marcasite in massive form. Volume Percentage Marcasite 20-25%, Porosity  $0.8 \pm 0.2\%$ . Locality: Pine Point, N.W.T.

PPG; Calcite Galena Sphalerite. Galena Sphalerite in massive form. Volume Percentage Sulphide 20-25%, Porosity  $0.5 \pm 0.2\%$ . Locality: Pine Point, N.W.T.

Hawk: Dolomite Galena. Galena in massive form. Volume Percentage Galena 10-15%, Porosity  $0.5 \pm 0.2\%$ . Locality: Hawk Creek, B.C.

LCI: Dolomite Marcasite Galena. Galena in massive form, Marcasite colloform. Volume Percentage Sulphide 10-15%, Porosity  $2.3 \pm 0.2\%$ . Locality: Little Cornwallis Island, N.W.T.

The results for these samples when saturated with tap water are shown in Figures 7a, 8a, 9a and 10a; results when saturated with 0.1 N sodium chloride solution are shown in Figures 7b, 8b, 9b and 10b.

Phase curves are shown for both 25°C and -14°C conditions, but amplitude curves are shown only for the 25°C case because of the variation that took place in the amplitude measurements at -14°C when a slight warming of the sample by the tank electrolyte was unavoidable. The phase curves for -14°C proved insensitive to this warming, as can be seen in the two sets of data values for -14°C in Figure 7b. These value sets were obtained several minutes apart, so that a noticeable change in the amplitude data due to warming was observed, yet the phase values displayed this satisfactory repeatability.

The individual behaviour of the mineral specimens as revealed by Figures 7, 8, 9 and 10 may be evaluated in the following way:

1. Variations of chargeability  $m$  cause vertical displacement of the whole of the phase curve, with increase of  $m$  causing elevation of the phase curve.
2. Variations of the time constant  $\tau$  displace the point of critical (or peak phase) frequency, with displacements toward lower frequency indicating an increase of  $\tau$ .

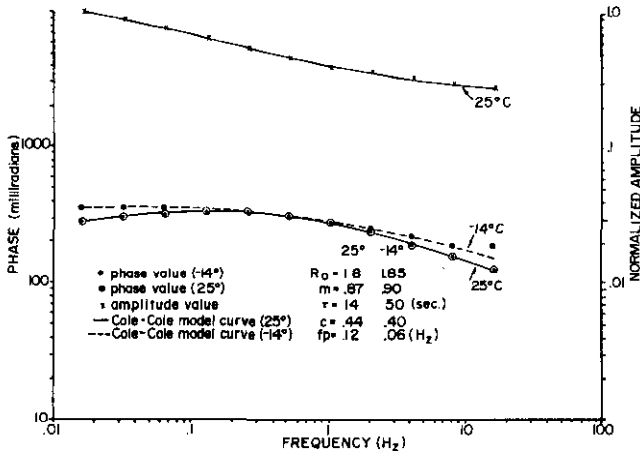


Fig. 7a. Frequency response of sample PPM with tap-water electrolyte at two temperatures.

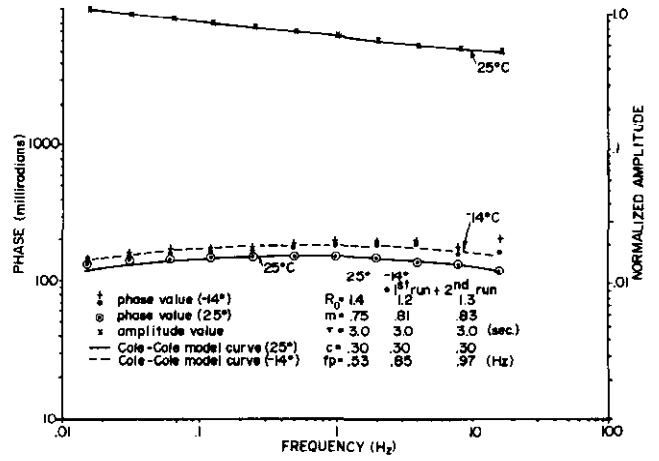


Fig. 7b. Frequency response of sample PPM with 0.1 N NaCl electrolyte at two temperatures.

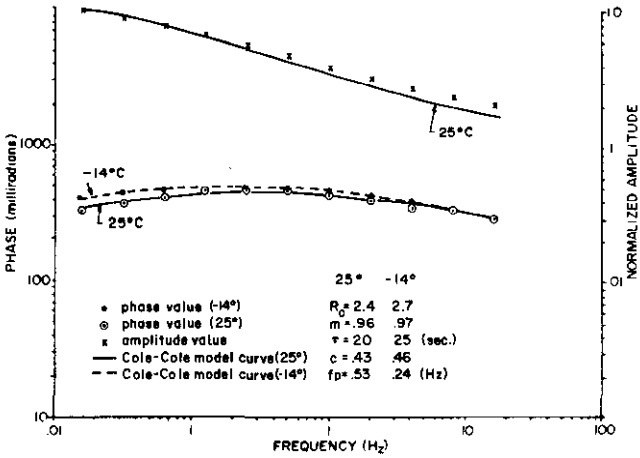


Fig. 8a. Frequency response of sample Hawk with tap-water electrolyte at two temperatures.

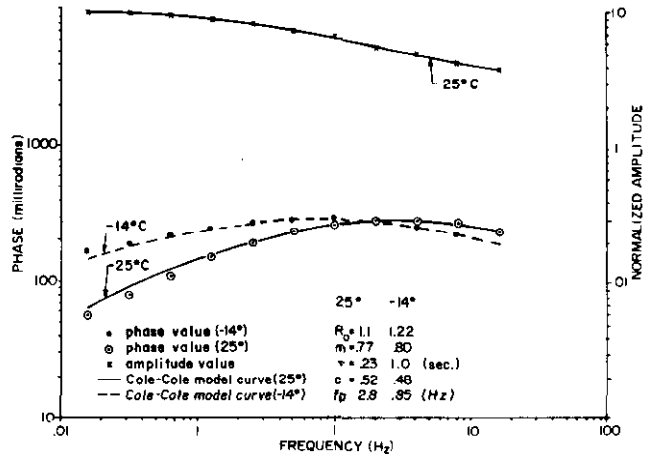


Fig. 8b. Frequency response of sample Hawk with 0.1 N NaCl electrolyte at two temperatures.

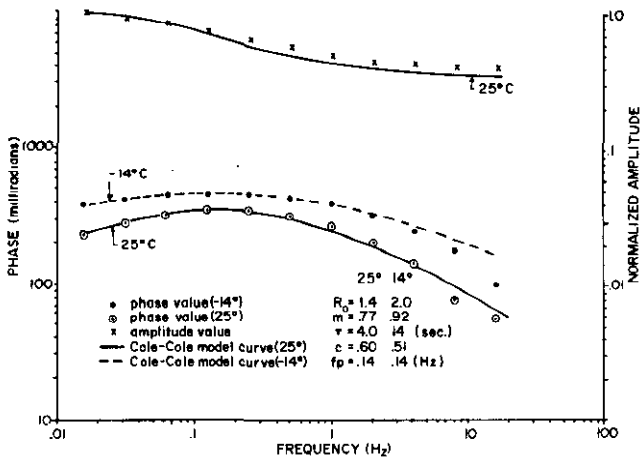


Fig. 9a. Frequency response of sample PPG with tap-water electrolyte at two temperatures.

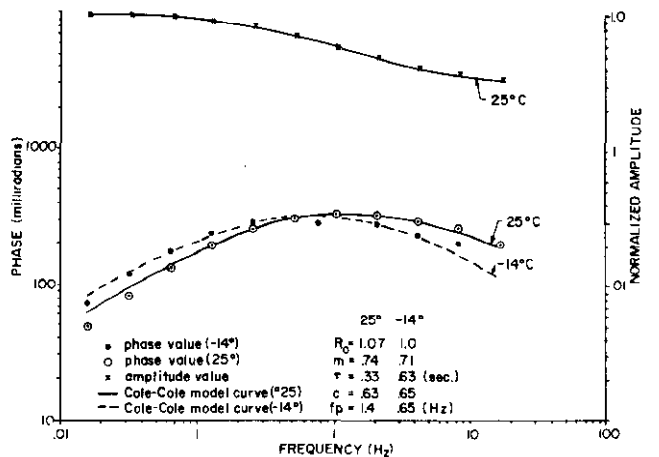


Fig. 9b. Frequency response of sample PPG with 0.1 N NaCl electrolyte at two temperatures.

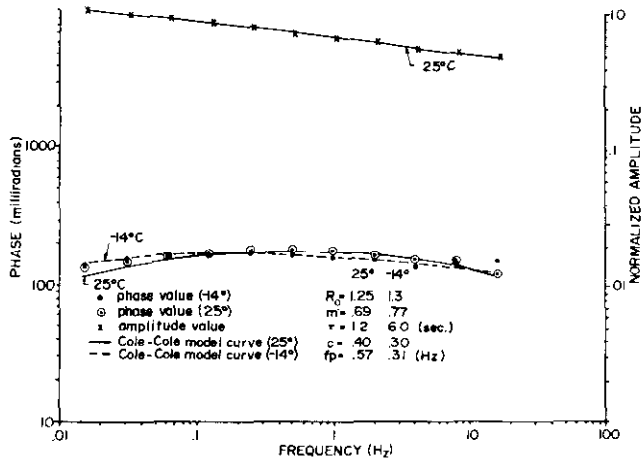


Fig. 10a. Frequency response of sample LCI with tap-water electrolyte at two temperatures.

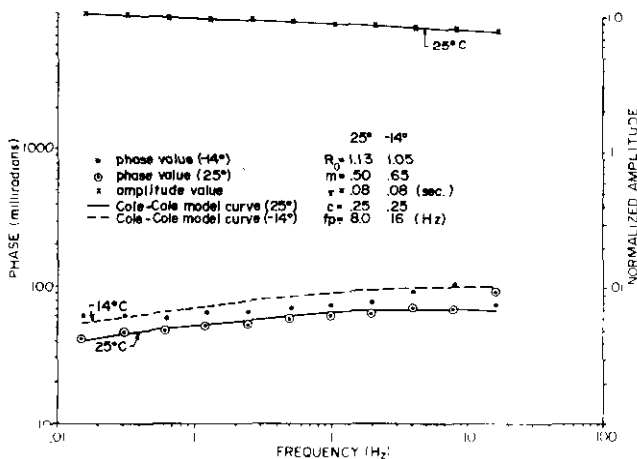


Fig. 10b. Frequency response of sample LCI with 0.1 NaCl electrolyte at two temperatures.

3. Any decrease of the frequency dependence  $c$  causes a decrease of the gradient of the phase curve on both sides of the critical frequency, *i.e.* it causes a general flattening.
4. Throughout these experiments the DC resistance values  $R_0$  were normalized with respect to the resistance at 0.0156 Hz, and the absolute values of the DC resistance of the samples were not measured. In cases where 0.0156 Hz fell on the slope of the amplitude curve, the derived value for  $R_0$  at zero frequency exceeded the value of 1.0.

The range of values for  $m$ ,  $\tau$  and  $c$  found in these experiments appears to agree with those found by Pelton *et al.* (1978) and Klein and Hallof (1982), the only disagreement being that the values measured for  $c$  were in general higher than the average of 0.25 found by Pelton *et al.* (1978) but in good agreement with the modal value of 0.4 found by Klein and Hallof (1982).

The trends in the changes that  $m$  and  $c$  showed in response to increase of salinity and reduction of temperature can be seen in the composite diagrams presented in Figures 11, 12 and 13.

The increase of salinity produced a clear depression of both  $m$  and  $\tau$  in all cases, but can only be said to have increased the scatter of  $c$  values.

The decrease of temperature produced a general trend toward higher values of chargeability  $m$  in both the low- and high-salinity cases shown in Figure 11. The maximum observed increase was 305 (LCI high salinity) while one case of decrease was observed (PPG - 4.2% high salinity).

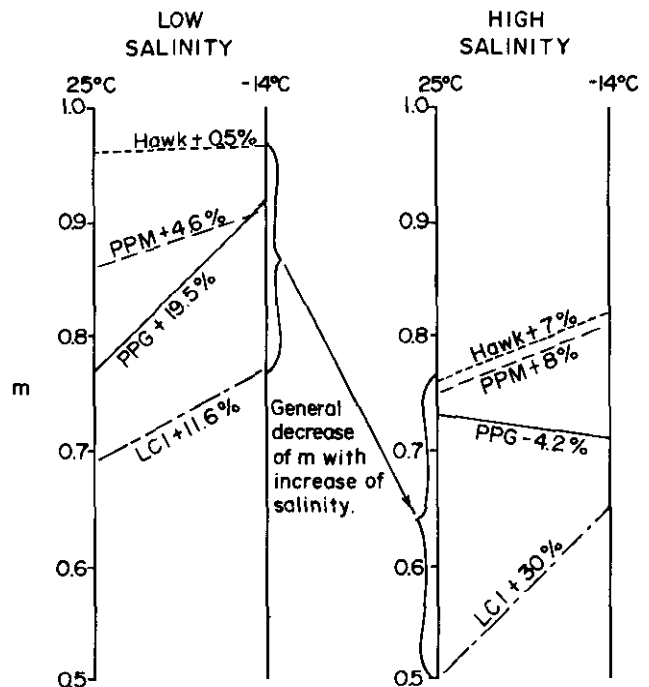


Fig. 11. Variation of chargeability ( $m$ ) with temperature and salinity.

Dramatic increases of time constant were observed in all four specimens as temperature was lowered for low-salinity conditions (Fig. 12). The mean increase under these conditions was 240% with a range from 25% to 400%. The trend for high-salinity conditions also appeared to be an increase as temperature was lowered; however, in two cases there was no change of  $\tau$ .

The frequency dependence  $c$  showed a general decrease with decrease of temperature under low-salinity conditions, but no dominant trend could be said to exist in the data for high-salinity conditions (Fig. 13).

The observed trends in the behaviour of  $m$  appear understandable in terms of relative changes in the resistance of so-called blocked and unblocked current paths in the rock. The equivalent unblocked path resistance was denoted  $R_0$  by Pelton *et al.* (1978) while the resistance equivalent to that of the paths blocked by metallic mineral was denoted  $R_1$ . The chargeability  $m$  was shown by these authors to be given by

$$m = R_0 / (R_1 + R_0)$$

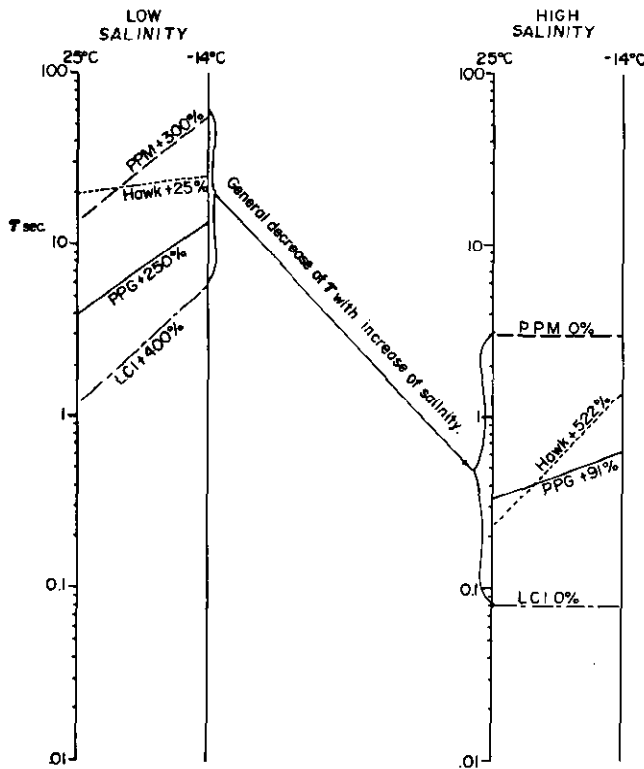


Fig. 12. Variation of time constant ( $\tau$ ) with temperature and salinity.

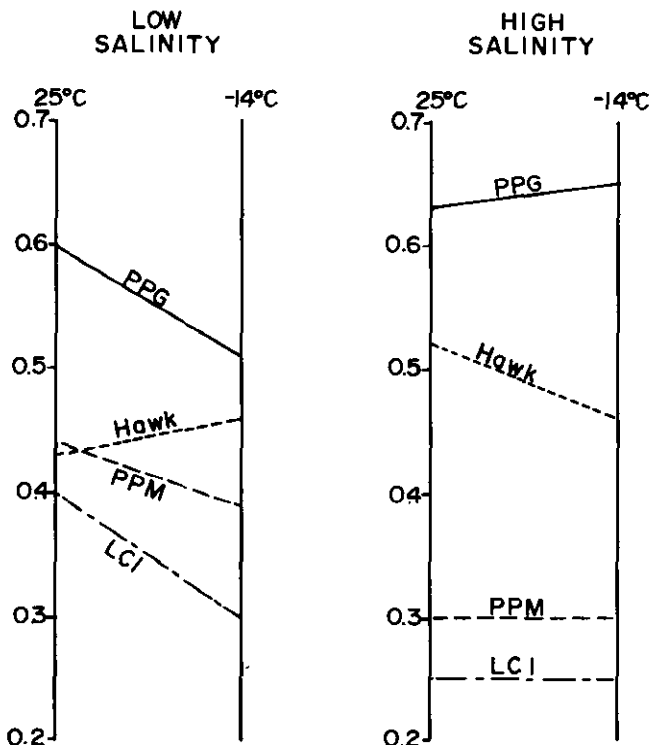


Fig. 13. Variation of frequency dependence ( $c$ ) with temperature and salinity.

We can surmise that  $R_0$  would be strongly dependent on pore-fluid salinity, but that  $R_1$  would be less sensitive to salinity because it would also include ohmic resistance at the mineral surface and within the mineral.

It therefore appears that increase of salinity would reduce  $R_0$  more than  $R_1$  and result in a decrease of the ratio  $R_0/(R_1 + R_0)$ .

The freezing of the pore fluid would probably not affect the contribution to  $R_1$  due to the mineral, so that  $R_0$  would increase more than  $R_1$ , thereby resulting in a tendency for the ratio  $R_0/(R_1 + R_0)$  to approach the theoretical maximum value of 1.0. The freezing of the rock can also be viewed as reducing its porosity. McEuen *et al.* (1959) found that, in synthetic rock specimens, a reduction of porosity produced an increase in the polarizability of such specimens, so we can see that the results obtained with frozen specimens are in accord with those results. The Cole-Cole model shows that it is the reduced influence of blocked pore paths as porosity is reduced that results in the rise of over-all chargeability.

The behaviour of  $\tau$  may be understood by considering the expression for  $\tau$  presented by Pelton *et al.* (1978):

$$\tau = X(R_0/m)^{1/c} = X(R_1 + R_0)^{1/c}$$

which for the case of  $c = 1$  becomes

$$\tau = X(R_1 + R_0)$$

and  $X$  can be recognized as being related to the capacitance of the frequency-dependent current paths in a rock.

An increase of salinity would reduce  $R_1$  and  $R_0$ , thereby reducing  $\tau$ , as was observed. However, it appears possible that an increase of salinity may also affect the charge-storing capacity of the metallic grain surfaces, in effect reducing  $X$ .

The observed rise of  $\tau$  with freezing appears to be readily explained by a rise of both  $R_1$  and  $R_0$ . This can be viewed in an alternative way, in that the formation of ice in pores will increase the path length that ions must traverse in attempting to re-establish equilibrium within a rock in response to a disturbance created by an imposed current. Variations of path length can be described by the tortuosity of rock, which Jackson *et al.* (1978) found to be strongly related to the exponent in Archie's Law. They found that, for constant porosity, an increase of tortuosity increased a rock's over-all resistivity, and this agrees with the observed increase of  $\tau$  which, in the Cole-Cole model, is dependent on resistivity represented by  $R_0$  and  $R_1$ .

Variations of the polarization characteristics of minerals have been related to mineral grain size by Pelton *et al.* (1978) and by DeWitt and Sill (1976). They found that, in general, measured values of time constant  $\tau$  show an increase with increase of mineral grain size, and are greatest for minerals showing a veinlet character. The definition of  $\tau$  in the Cole-Cole model (*i.e.*  $\tau = X(R_1 + R_0)^{1/c}$ ) indicates that, for a fixed value of  $c$ , large values of  $\tau$  will be generated by large values of  $X$  or of  $R_1$

and  $R_0$ . In that  $R_1$  and  $R_0$  are related to pore-path length, it is possible to ascribe the high values of  $\tau$  observed by these authors to a large path length in the large grain or veinlet cases. In this sense it appears that large  $\tau$  values can be related to a rock texture that accompanies large grains or veinlets. It also appears that freezing tends to produce a texture of this type in any rock. Equally well, the observed large  $\tau$  values may be caused by large values of  $X$ , but we can not say how freezing may affect  $X$ .

A comparison of the results shown in Figures 12 and 13 shows a strong correlation between the behaviour of  $\tau$  and of  $c$ . The expression relating  $\tau$  and  $c$  (i.e.  $\tau = X(R_1 + R_0)^{1/c}$ ) shows that, for fixed values of  $X$ ,  $R_1$  and  $R_0$ , a decrease of  $c$  will produce an increase of  $\tau$ , and that small values of  $c$  will be associated with large values of  $\tau$ . On this basis it is possible to predict that in the low-salinity case the variations of  $c$  shown in Figure 12 should lead to increases of  $\tau$  with freezing that, in order of magnitude, should be LCI greatest, PPM, PPG and Hawk smallest — as, in fact, is shown by Figure 12. The behaviour of  $c$  for the Hawk sample would predict a decrease of  $\tau$ , but this would happen only if  $R_1$ ,  $R_0$  and  $X$  did not vary. The notably small increase of  $\tau$  for the Hawk sample appears due to the conflict between the increase in  $\tau$  due to increases in  $R_1$  and  $R_0$ , and the decrease in  $\tau$  due to the increase of  $c$ .

In a discussion of  $c$ , DeWitt and Sill (1976) indicated that values of  $c$  close to 0.5 were associated with metallic mineral content of the sample which displayed a single grain size. When a dispersion of grain sizes of metallic mineral was present, the value of  $c$  approached 0.25. This could be taken to mean that  $c$  depends only on the distribution of grain sizes of the metallic mineral but, if this was the case, the freezing of the sample should not produce any change in  $c$ . Such was clearly not the case, and it appears that  $c$  should be related not only to metallic-mineral grain-size distributions but also to pore geometries that inevitably accompany these distributions. Until a specific study is made of this point, it is entirely possible that the association between  $c$  and pore geometry is the primary association, and that between  $c$  and metallic-mineral grain size is secondary.

The results of this study indicate that  $\tau$  is dominantly controlled by  $R_1$  and  $R_0$ , but that  $c$  also can have a strong influence on  $\tau$ . Whereas the behaviour of  $R_1$  and  $R_0$  is readily explained in relation to the freezing of the sample, it is difficult to provide an explanation for the behaviour of  $c$  other than to say it is not controlled by metallic-mineral grain size. A possible hypothesis for of the behaviour of  $c$  and  $\tau$  is that  $\tau$  predominantly reflects path length whereas  $c$  reflects uniformity of the pore system in a rock, with  $c = 0.5$  indicating high uniformity and  $c = 0.25$  low uniformity. The formation of ice in pores will probably degrade the uniformity in most cases, thereby reducing  $c$  with a consequent increase of  $\tau$ .

A practical consequence of this study is that it is possible to predict that time domain IP surveys may detect very high polarization effects over frozen mineral bodies because of the type of parameter normally measured in such surveys. This parameter is the integral chargeability  $M$ , the definition of which is shown in Figure 14 as being the area under the time domain IP decay curve. This parameter is directly proportional to both  $m$  and  $\tau$ , so that if both  $m$  and  $\tau$  increase on freezing, the resultant measured values of  $M$  will show a rise that reflects the product of  $m$  and  $\tau$ , with the consequence that very dramatic increases of  $M$  may be seen.

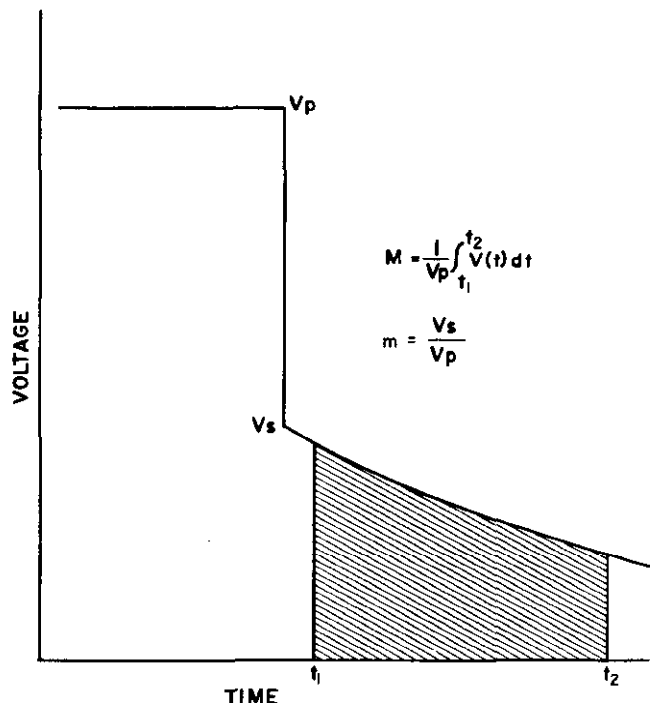


Fig. 14. The chargeability  $M$  defined as the area over a definite time interval of the transient decay curve.

## CONCLUSIONS

As a result of this study it appears possible to predict that, in general, mineralized rocks when frozen will show an enhancement of both chargeability  $m$  and time constant  $\tau$ , regardless of mineral type or texture. The frequency dependence  $c$  will generally show a decline on freezing, except when highly saline pore fluids are present.

It appears probable that these general conclusions can be applied to frozen minerals *in situ*, and that field measurements over frozen mineralized rocks by means of time domain IP surveys may show very large values of the integral chargeability when compared with measurements made over unfrozen rocks.

## REFERENCES

- DeWitt, G. and Sill, W.R. 1976. Parametric studies of IP spectra. Presented at the 46th Annual International SEG Meeting, October 26 in Houston.
- Jackson, P.D., Taylor Smith, D. and Stanford, P.N. 1978. Resistivity - porosity - particle shape relationships for marine sands. *Geophysics*, v. 43, p. 1250-1268.
- Kay, A.E. 1981. The Effects of Low Temperature on the Induced Polarization Response of Mississippi Valley-type Ore Samples. Unpublished M.Sc. thesis, Department of Geology and Geophysics, The University of Calgary, 121p.
- Klein, J.D. and Hallof, P.G. 1982. Electrical properties of metallic mineral deposits of Ontario. Presented at the 52nd Annual International SEG Meeting, October 17-21, Dallas, Texas.
- McEuen, R.B., Berg, J.W. Jr. and Cook, K.L. 1959. Electrical properties of synthetic metalliferous ore. *Geophysics*, v. 24, p. 510-530.
- Pelton, W.H., Ward, S.H., Hallof, P.G., Sill, W.R. and Nelson, P.H. 1978. Mineral discrimination and removal of inductive coupling with multifrequency IP. *Geophysics*, v. 43, p. 588-609.
- Van Voorhis, G.D., Nelson, P.H. and Drake, T.L. 1973. Complex resistivity spectra of porphyry copper mineralization. *Geophysics*, v. 38, p. 49-60.
- Zonge, K.L., Sauck, W.A. and Sumner, T.S. 1972. Comparison of time, frequency and phase measurements in induced polarization. *Geophysical Prospecting*, v. 20, p. 626-648.